Interaction of novel proteins, centrin4 and protein of centriole in Leishmania parasite and their effects on the parasite growth

Kavita Vats, Rati Tandon, R. Roshanara, Mirza A. Beg, Rosa M. Corrales, Akila Yagoubat, Enam Reyaz, Tasaduq H. Wani, Mirza S. Baig, Ashok Chaudhury, et al.

Interaction of novel proteins, centrin4 and protein of centriole in *Leishmania* parasite and their effects on the parasite growth

Kavita Vats [a, b, e, 1], Rati Tandon [a, 1], Roshanara [a, 1], Mirza.A. Beg [a], Rosa M. Corrales [e], Akila Yagoubat [e], Enam Reyaz[a], Tasaduq.H. Wani [a], Mirza.S. Baig [a], Ashok Chaudhury [b], Anuja Krishnan [a], Niti Puri [c], Poonam Salotra [d], Yvon Sterkers[e], Angamuthu Selvapandiyan [a,*]

[a] Department of Molecular Medicine, Jamia Hamdard, New Delhi 110062, India, [b] Department of Bio & Nano Technology, Bio & Nano Technology Centre, Guru Jambheshwar University of Science and Technology, Hisar 125001, India, [c] School of Life Sciences, Jawaharlal Nehru University, New Delhi 110067, India, [d] ICMR-National Institute of Pathology, Safdarjung Hospital Campus, New Delhi 110029, India, [e] MiVEGEC, University of Montpellier, CNRS, IRD, Academic Hospital (CHU) of Montpellier, Montpellier 34295, France

* Corresponding author. *E-mail address:* selvapandiyan@jamiahamdard.ac.in (A. Selvapandiyan). [1] Contributed equally to this work.

This manuscript has been published and is also available in: Interaction of novel proteins, centrin4 and protein of centriole in *Leishmania* parasite and their effects on the parasite growth. Vats K, Tandon R, Roshanara, Beg MA, Corrales RM, Yagoubat A, Reyaz E, Wani TH, Baig MS, Chaudhury A, Krishnan A, Puri N, Salotra P, **Sterkers Y**, Selvapandiyan A.Biochim Biophys Acta Mol Cell Res. 2023 Mar;1870(3):119416. doi: 10.1016/j.bbamcr.2022.119416. Epub 2023 Jan 7. PMID: 36623775

ABSTRACT

Centrins are cytoskeletal proteins associated with the centrosomes or basal bodies in the eukaryotes. We previously reported the involvement of Centrin 1–3 proteins in cell division in the protozoan parasites *Leishmania donovani* and *Trypanosoma brucei*. Centrin4 and 5, unique to such parasites, had never been characterized in *Leishmania* parasite. In the current study, we addressed the function of centrin4 (LdCen4) in *Leishmania*. By dominant-negative study, the episomal expression of C-terminal truncated LdCen4 in the parasite reduced the parasite growth. LdCen4 double allele gene deletion by either homologous recombination or CRISPR-Cas9 was not successful in *L. donovani*. However, CRISPR-Cas9-based deletion of the homologous gene was possible in *L. mexicana*, which attenuated the parasite growth in vitro, but not ex vivo in the macrophages. LdCen4 also interacts with endogenous and overexpressed LdPOC protein, a homolog of centrin reacting human POC (protein of centriole) in a calcium sensitive manner. LdCen4 and LdPOC binding has also been confirmed through in silico analysis by protein structural docking and validated by co-immunoprecipitation. By immunofluorescence studies, we found that both the proteins share a common localization at the basal bodies. Thus, for the first time, this article describes novel centrin4 and its binding protein in the protozoan parasites.

Keywords: Centrin protein Protein of centriole Protein interaction *Leishmania donovani* Basal bodies

Abbreviations: LdCen4: *Leishmania donovani* centrin 4, LdPOC: *Leishmania donovani* protein of centriole, LmxCen4: *Leishmania mexicana* centrin 4, hPOC: human protein of centriole, CRISPR: clustered regularly interspaced short palindromic repeats, GST: Glutathione S-transferase

1. Introduction

Highly conserved calcium-binding cytoskeletal proteins unique to eukaryotes, Centrins are localized in the microtubule-organizing center [1,2]. They play regulatory roles in the duplication or segregation of the centrosome or basal bodies in the eukaryotes [3,4]. By means of its Ca2+-binding property, centrin represents a unique quality of translocation regulation of signaling proteins in sensory cells, suggesting a possible link between molecular trafficking and signal transduction [5]. Centrin isotypes have been reported in many organisms, with three in humans and four in mice [3,6]. Among the divergent eukaryotes, 4 centrin isotypes are described (PfCen1–4) in *Plasmodium falciparum* [7] and 5 in *Leishmania* spp. (LmCen1–5) and *T. brucei* (TbCen1–5) [8,9]. Centrin 1–3 in *T. brucei* and *Leishmania* are found to be similar to human centrin1–3 having EF-hands I and IV as two putative calcium-binding sites [1,8]. LmCen4 and TbCen4 (accession numbers: LmjF32.0660; XP_829446 respectively) have putative calcium-binding EF I/III hands, whereas LmCen5 and TbCen5 (accession numbers: LmjF36.6110; XP_823096 respectively) do not have any putative calcium-binding EF- hands [1,8]. Both centrin4 and centrin5 are unique to the Trypanosomatidae family. Amastigote-specific genes (ASGs), significantly involved in parasite pathogenesis, its physiology and essential for its survival inside the macrophages, need to be characterized prior to developing live attenuated vaccine cell lines by deletion of such genes [10]. In the past, double allelic deletion of centrin1 (LdCen1)

in *Leishmania donovani* [4] caused growth attenuation selectively in the intracellular amastigote stage of the parasite in vitro as well as in vivo in animals [4,11]. Knockout of centrin1 in *L. donovani* particularly affected cell cytokinesis in the amastigotes, generating multinucleated cells and eventually causing their cell death in vitro and in vivo [4,11]. Such parasite as a vaccine candidate also exhibited safety, immunogenicity and protection against wild-type parasite infection in rodents and canine models [11–14]. Characterization of protein towards a better understanding of parasite biology largely involves identifying its binding partners that could regulate its specific function. Similarly, centrin interaction with other proteins is known. The Saccharomyces cerevisiae centrin, Cdc31p, bind- ing partner Sfi1p possess conserved binding sites to centrin and are indispensable in spindle pole body duplication [15]. Another instance, is where the interaction of Centrin2 with the protein of Xeroderma pig- mentosum group C reportedly stimulates the nucleotide excision repair in Saccharomyces cerevisiae [16]. Overexpression of the interacting protein POC5 (LdBPK_362830.1) directs the assembly of linear, centrin- dependent structures that employ other centriolar proteins, viz. peri- centriolar material 1 (PCM-1) and NEDD1 [17]. The putative centrin, LdCen4, having the longest N-terminal extension among the centrins is unique to the parasite and has never been functionally characterized. Here, we have attempted to characterize LdCen4 and exemplify its role in the cell biology of the parasite by creating a null mutant via the CRISPR Cas9 approach. Furthermore, a human homolog of a conserved novel centrin binding protein, hPOC5, similar to Sfi1p in *L. donovani*, called LdPOC, has been identified and characterized. The interaction of LdPOC with centrin4 has been assessed by in vitro as well as by in silico approaches.

2. Materials and methods

2.1. *Leishmania* strain and culture conditions

Promastigotes and axenic amastigotes of *L. donovani* 1S (a cloned line from strain 1S, WHO designation: MHOM/SD/62/1S) and *L. mexicana* T7Cas9 strain [18] were cultured at 27 ◦C in M199 based medium as reported earlier [19,20].

2.2. Cloning, expression and purification of LdCen4 protein in E. coli

The genomic DNA of *L. donovani* was used to PCR amplify the ORF of the LdCEN4 gene fused with 6 His tag, using primers Cent4 6F CT Topo and Cent4 7R CT Topo (Supplementary Table 1). Further subcloning of LdCEN4, expressing in the bacterium Escherichia coli, purifying the protein and raising polyclonal antibodies in rabbits (produced and confirmed its specificity by GeNei, Bangalore, India) were as previously described by us [1,19].

2.3. Cloning and expression of full length and mutant forms of LdCen4 in *Leishmania* expression vector

To express the full-length and mutant form of LdCen4 in *L. donovani*, wild-type and truncated ORFs were PCR amplified containing hemagglutinin (HA) tag sequence at the C-terminal followed by SpeI restriction site (bold) with the primers as in the Supplementary Table 1. The PCR amplified products were initially cloned into a pGEMT-Easy T/A cloning vector, and the authenticity of the constructs was established by Sanger sequencing. The sequence confirmed insert was excised as a SpeI frag- ment and cloned at the same site of pKSNeo [21]. The orientation of the gene in the pKSNeo vector was confirmed by forward primer 13F pKSNeo (Supplementary Table 1) and a gene-specific reverse primer sequence as mentioned in (Supplementary Tables 1 & 2). Mid-log phase promastigotes were harvested and transfected with the above constructs as described earlier [22]. Parasites transfected with vector alone were used as control.

2.4. Immunofluorescence analysis

To know centrin protein localization, the promastigotes and axenic amastigotes of *L. donovani* were harvested from the mid-log culture, allowed to attach to the poly L-lysine coated coverslip, fixed in 4 % PFA (paraformaldehyde) and processed for immunofluorescence analysis as described earlier [4,8]. The primary antibodies used were anti-LdCen4 (1:500), anti-HA (1:500) (Sigma) antibody and the secondary anti- bodies used were Alexa Fluor® 633 Goat anti-Mouse IgG (H + L) (1:500) and Alexa Fluor® 488 Goat anti-rabbit IgG (H + L) (1500) [8].

2.5. Cell cytoskeleton preparation

Cell cytoskeleton was prepared with modification of a recent pro- tocol [23]. Briefly, the cells were harvested, washed with 1 ml PBS and then centrifuged at 800g for 5 min at 4 ◦C. The cell pellet was resus- pended in the 300 µl of cytoskeletal extraction buffer (100 mM Pipes pH 6.8, 1 mM MgCl2, 1%NP40) in ice for 7 min and centrifuged at 800g for 5 min at 4 ◦C. The supernatant contained all the cytoskeletal proteins that were subjected to Western blotting.

2.6. CRISPR CAS9-based deletion of Centrin4 gene in *L. mexicana*

Our initial experiments to delete centrin4 gene by either double homologous recombination [4] or CRISPR Cas9 [18] based approaches in *L. donovani* did not yield a viable parasite (data not shown). Hence, based on reported gene deletions by CRISPR Cas9 procedure in *L. mexicana* parasite, we attempted to delete homologous centrin4 gene (LmxCen4) by the same procedure in *L. mexicana*. Primers for deleting the target gene LdCen4 were designed using LeishGEdit software [18] and mentioned in Supplementary Table 3. To delete the target gene, two sgRNAs were PCR amplified using primer combination LmxC4 5′SgRNA/SgRNA reverse universal and LmxCen4 3′SgRNA/SgRNA reverse universal, to use to cut at the sites immediately upstream (5′) and downstream (3′) of the target gene. Donor DNA with drug-selectable marker genes (neomycinR and puromycinR) flanking nucleotides specific to the target gene was PCR- amplified using pT-Neo and pT-Puro plasmids [18] with primer LmxCen4 1 UFP (Upstream forward primer) and LmxCen4 2 DRP (Downstream reverse primer) (Supplementary Table 3) designed through LeishGEdit site. LmxT7Cas9 cells were grown in the exponential phase in a T25 cm^2 flask containing M199 medium along with Hygromycin for a minimum of one week until the day of transfection. For gene knockout, 1 × 107 cells were taken and washed in the 3×Tb-BSF buffer [24]. Cells were resuspended in 1xTb-BSF buffer [25 µl CaCl2: 83 µl of 3× Tb-BSF: 92 µl H20] in a total volume of 250 µl with 50 µl of PCR purified SgRNA and donor DNA mix, transferred into electroporation cuvette and transfected with one pulse with X-001 in Amaxa Nucleofector 2b [18]. Transfected cells were transferred into a pre-warmed medium and left to recover for one day before adding antibiotics and the clonal lines were obtained by serial dilution approach. Survival of drug-resistant transfectants became apparent in less than a week after transfection. The selected clonal lines were tested for the absence of the gene by PCR and by Western blot analysis as carried out earlier [4]. For the immunoblot analysis, the cells were lysed and subjected to SDS-PAGE, and the resolved proteins were transferred to the PVDF membrane and probed with an anti-LdCen4 antibody.

2.6.1. Cloning and expression of LdPOC

hPOC5 is a known centrin binding protein in humans [25]. The sequence of hPOC5 of humans was retrieved from NCBI by searching with accession number NP_001092741.1 (human). This sequence was subjected to BLAST analysis against the *L. donovani* genome to identify its homolog in *Leishmania*, which is a conserved hypothetical protein (LdPOC). Gene sequence was retrieved from NCBI for the LdPOC gene. For gene cloning, primers were designed with BamHI restriction site in forward primer and SalI restriction sites in reverse primer (Supplementary Table 4). The LdPOC gene (Accession number: XP_003865398.1) was PCR amplified and cloned in the pGEMT vector (Promega) using T4 DNA ligase. The positive clones screened by colony PCR and restriction digestion were further subcloned into the pGEX-6P2 vector (Novagen). Such vector transformed *E. coli* cultures were induced for the protein expression with IPTG and analyzed by SDS-PAGE as above in section 2.2.

2.6.2. Development of LdPOC-HA overexpressing L. donovani parasite

The LdPOC gene was amplified using specific primers with N-ter- minal SpeI restriction sites and HA tag nucleotide sequence in the reverse primer (Supplementary Table 4) from *L. donovani* DNA by PCR. The protein expression in the parasite through pKSNEO vector was done similarly as in the case of Centrin1-HA overexpression [1].

2.6.3. LdPOC and LdCen4 interaction by pull-down assay

The recombinant Glutathione S-transferase (GST)-LdPOC fused protein purified from E. coli was conjugated with Glutathione–sepharose beads followed by incubation of such beads with *L. donovani* parasite lysate for LdPOC to interact with endogenous LdCen4. The final beads were processed for SDS-PAGE followed by Western blot analysis as per published protocol [26] using α-LdCen4 Ab or α-GST antibodies. Recombinant GST protein alone expressed in the bacterium was also used similarly as an assay control. For the pull-down assay involving the use of Ca2 , the rLdPOC conjugated GST beads were washed with Ca2+ free (10 mM ethylenediaminetetraacetic acid [EDTA] in wash buffer pH 7.4) or Ca2+ containing (10 mM EDTA, 35.6 mM CaCl2 in wash buffer pH 7.4) buffer. After washing, the beads were supplemented with purified rLdCen4 protein for 1 h on a rocking platform at 4 ◦C with a final protein concentration of 5 µg/ml. The rest of pull-down of proteins in the presence or absence of Ca2+ was as described earlier [26]. Binding interaction between the proteins was confirmed through Western Blot using αLdCen4 antibodies.

2.7. In silico interaction between LdCen4 and LdPOC

2.7.1. Template identification for POC protein of L. donovani

Phyre2 tools performed protein structure prediction by fragment assembly to predict the 3D structure of POC protein of *L. donovani*. In the first step, the PSI-BLAST alignment was performed to find the suitable templates for modelling POC protein, which returned 865 UniRef se- quences like the query sequence. Based on the score (158), E-value (2e-37) and percentage similarity (94.7 %), the UniRef50 ID:

Q4Q1F1 sequence was shortlisted for model building.

2.7.2. Model building and structural validation

The UniRef50 ID: Q4Q1F1 sequence was compared with well- characterized protein structures available in the protein databank (PDB). The multiple PDB protein templates (100) were detected by HHpred

1.51, and secondary structure prediction was performed by Psi- pred 2.5. The unannotated region of the modelled protein was predicted by Disopred 2.4. Twenty successful 3D models of POC protein were generated by Phyre2 tools after 100 iterations. Phyre2 modelling is completed into seven steps-energy calculations, Helix-Sheet-Loop refinement, model building, simulated annealing, loop modelling, Backbone Root Mean Square Deviation calculation (RMSD), and finally assembling and ranking of the final model according to minimum energy [27]. The RMSD between the target and template protein was calculated, and TM- score, a normalized score varying from 0 to 1, stands for overall similarity between the target and template proteins and evaluated. Highly similar models have a TM-score > 0.7, same fold >0.5 and different folds <0.5. The Ramachandran plot (RP) analysis was per- formed for structure validation of modelled protein through the SWISS-MODEL structure assessment server [28].

2.7.3. Docking of LdCen4 protein with LdPOC protein of L. donovani

Docking of Centrin4model.pdb (as a receptor) with POC model.pdb (as a ligand) was performed by ZDOCK version 2.3.2 (http://zdock. umassmed.edu/) Fast Fourier Transform based protein docking Algo- rithm. The grid size for receptor protein was 20.488, 45.453, 11.842, and for ligand, the coordinates (X, Y, Z) for the grid were 45.669, 42.966, 19.779 (all distances in Å). ZDOCK searches all potential binding modes in the translational and rotational space between the proteins and assesses each pose using an energy-based grading function. The scoring functions consist of Atomic Contact Energy (ACE) Statistical Potential, Shape Complementarity, and Electrostatics. The ZDOCK output lists the top 10 potential docked complexes sorted by rank, 3 rotational angles and 3 translational parameters.

2.7.4. Analysis of docked complex

The amino acid residues directly implicated in the interaction of the LdCen4 model.pdb (as a receptor) with the LdPOC model.pdb (as a ligand) was analyzed using the DIMPLOT module of LigPlot version 1.4.5 [29]. Different types of bonds viz., hydrogen bond, hydrophobic interaction and double/triple bonds between docked complexes were found by DIMPLOT and visualized in the PyMOL Molecular Graphics System, Version 2.0 (Schro¨dinger, LLC). The interaction of LdCen4 with LdPOC was also confirmed using Alfpha fold and Robetta as described separately in the 'supplemental section'.

2.8. Statistics

The significant differences between the means of the groups were determined by a two-sample t-test assuming unequal variance using GraphPad Prism version 9. A p-value of 0.05 was considered highly significant.

3. Results

3.1. LdCen4 clusters together with LmxCen4

The obtained protein sequence of LdCen4 through the sequencing of our cloned ORF showed an identity of 94.6 % with Centrin4 of L. major and 92.34 % with that of *L. mexicana*. However, only 34.13 % sequence identity was observed with *L. donovani* calmodulin (LdCal; another calcium-binding protein), suggesting closeness of the protein to centrins. Comparing the sequence of LdCen4 with the homologs of other Try-panosomes and LdCal by ClustalW analysis, we identified two putative calcium-binding sites, i.e., EF-hand I and EF-hand III (due to occurrence of negatively charged amino acids: aspartic acids and glutamic acids), although LdCal displayed all 4 EF-hands (Fig. 1A). The online motif prediction software "myhits" [30] and the InterProScan Search Result (EMBL-European Bioinformatics Institute) [31] also predicted EF I and EF III (with maximum scores 13 and 19 respectively for the EF hands) as highly calcium binding notiffs. Through evolutionary tree analysis, both LdCen4 and LmxCen4 were grouped, and these two were placed distantly with LdCen1 but far distantly with LdCal (Fig. 1 B).

3.2. LdCen4 exhibits comparable protein expression at promastigote and amastigote stages

Recombinant centrin4 protein of *L. donovani* (rLdCen4; rC4), containing a HA tag, with a molecular weight of ~24 kDa, was expressed and purified from E. coli (Fig. 2A). Polyclonal antibodies raised against this protein in rabbits were used in subsequent studies. To find out the expression comparison of LdCen4 between promastigotes and axenic amastigotes, Western blot analysis was carried out, which indicated no significant difference in the levels of LdCen4 protein between the two stages of the parasite both at the log and stationary stages in cultures (Fig. 2B).

.

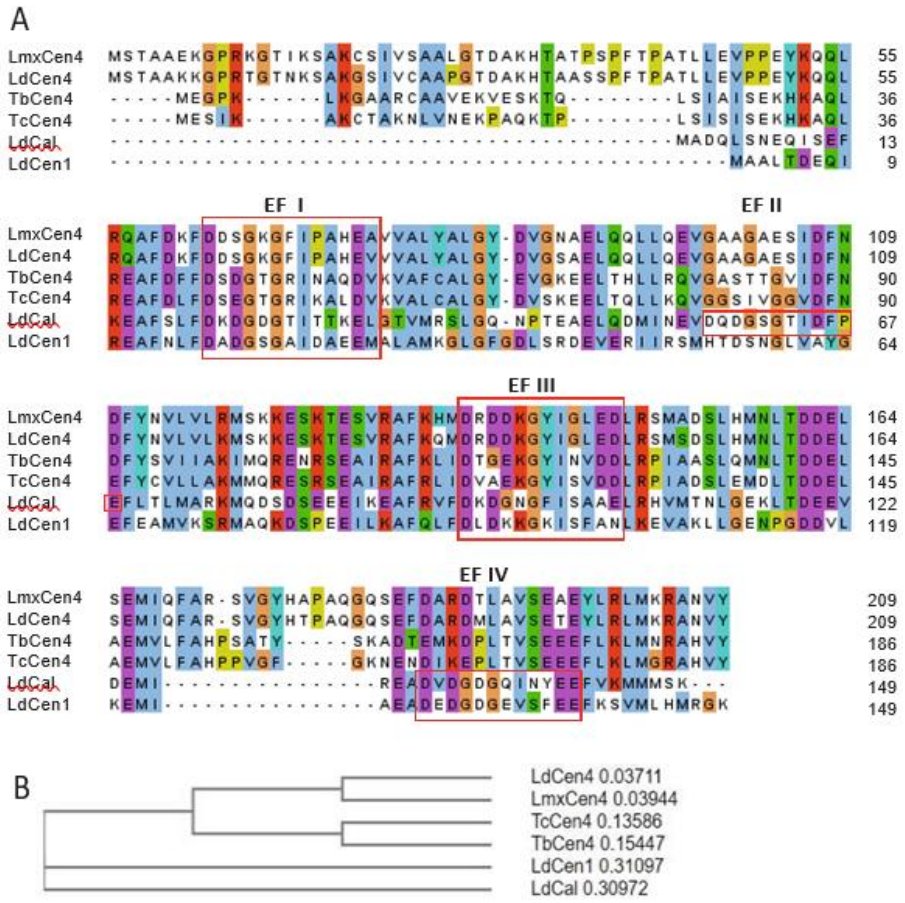

Fig. 1. LdCen4 sequence analysis.

A. Multiple alignment of Centrin4 protein sequences of *L. mexicana*, LmxCen4 (LmxM.31.0660), *L. donovani*, LdCen4 (LdBPK_320690.1), *T. brucei*, TbCen4 (Tb927.11.13900) and Trypanosoma cruzi, TcCen4 (TcCLB.509161.40), *L. donovani* centrin1, LdCen1 [1] and *L. donovani* calmodulin, LdCal (LdBPK_090970.1). The accession numbers are from www.tritrydb.org. The alignment was generated utilizing Jalview program version 2.11.2.4. The standard one-letter code is used to define amino acids. The boxes EF-hands: EF I (N-terminal) and EF IV (C-terminal) are the putative Ca2 + bind- ing domains. The colored patches indicate the respective stretch of amino acids' similarities among the sequences. B. Phylogenetic analysis of protein se- quences of Centrins mentioned above and *L. donovani* calmodulin by Neighbor-Joining distance analysis [32] using the online program ClustalW version 1.2.4

3.3. Immunofluorescence analysis (IFA) revealed subcellular localization of LdCen4 in the parasite

The immunofluorescence analysis of the promastigote cells of the parasite using anti- LdCen4 antibodies generated in rabbits revealed LdCen4 localization close to the kinetoplast at the basal body region and at the lobe-like structure(s), close to the basal body. This was confirmed in the same IFA by including known basal body reacting anti-YL1/2 antibodies [8] that co-localized LdCen4 only in the basal body region (Fig. 2C). The results suggest that LdCen4 protein may be closely associated with the regions of the basal body and lobe-like structure(s).

3.4. Episomal expression of C or N,C-terminals deleted LdCen4 display slowed-growth of the parasite

The LdCen4 mutant constructs (LdCen4 protein deleted for N-ter- minal, NEX- [extended N] terminal, C-terminal or N & C-terminals) (Fig. 3A) were transfected in the parasite to study the function of the LdCen4 gene via observation of changes in phenotype due to possibly a dominant-negative effect. The expression of all mutant proteins in the parasite was confirmed by an anti-HA antibody (Fig. 3B). The dark bands in the lanes close to the bands of interest (not with the N-terminal truncated protein expressions) could be due to post-transcriptional modifications. Such additional signals were absent along with the endogenous proteins in the Western blot (Fig. 2B). These observations need additional studies to clarify. The growth of the recombinant pro- mastigote parasites that express episomally, the full-length and the truncated form of LdCen4 mutants, were analyzed at 200 μg ml-1 of G418 (neomycin) (Fig. 3C). The parasite lines that expressed the full- length form of LdCen4 showed the same growth rate as the control, transfected with only the vector pKSNeo. The rest of the mutant protein- expressing parasites showed a comparatively slower growth rate than the controls. Especially, when we overexpress either C-terminal deleted, or NC-terminal deleted LdCen4 in *Leishmania*, we noticed a reduced growth rate of the parasite compared to control (Fig. 3D). This suggests that the C-terminal end of the LdCen4 gene might be crucial for the parasite's cell biology.

3.5. LmxCen4KO axenic amastigotes exhibited compromised growth in vitro but not ex vivo

3.5.1. CRISPR Cas9-based Centrin4 gene deletion in L. mexicana

Upon knowing the importance of LdCen4 protein to *L. donovani* through the above growth study of the promastigotes episomally expressing the truncated proteins, we aimed to see the physiology of the

parasites deleted for LdCen4 initially by the double homologous recombination approach [4]. However, by the conventional gene deletion approach [4], we could achieve only deletion of single allele KO in the parasite using hygromycin resistant gene construct and were unable to delete the second allele with the other neomycin resistant gene construct in *L. donovani*. The single allele KO cells neither show any growth defect nor change in their other physiology, e.g., morphology under microscopy (data are not shown). Our other attempt to carry out the deletion of LdCen4 via CRISPR Cas9 also failed (data not shown). However, while attempting to delete the homologous gene (LmxCen4) in *L. mexicana*, we could achieve a null mutant in this species. The results are as shown below.

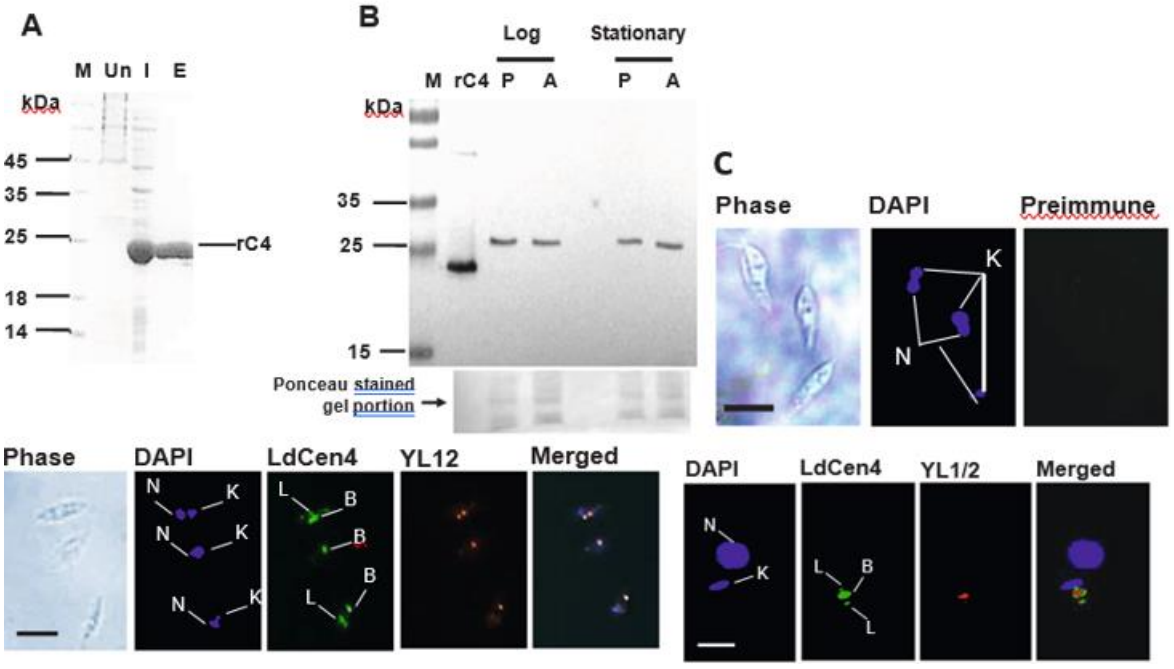

Fig. 2. Expression of recombinant LdCen4 protein in E. coli:

A. Coomassie-stained SDS PAGE gels showing the purified recombinant proteins of LdCen4 in E. coli. M: Marker UI: uninduced; I: induced and E: the eluted pure recombinant LdCen4 (rC4). B. Expression level of LdCen4 in the parasite life forms: Expression of LdCen4 proteins in the promastigotes (P) and axenic amastigotes (A) using anti-LdCen4 Ab. Lower panel: Ponceau stained gel pic- ture of part of the blot analyzed, showing the amount of proteins loaded in gel. C. Immunolocalization of LdCen4 protein in the parasite: IFA with preimmune serum as control is seen in the upper panel. Immunolocalisation of LdCen4 in the promastigotes of *L. donovani* (group of parasites in the middle panel and a different single-cell enlarged in the lower panel) using anti-LdCen4 Ab (green) and known basal body localizing anti-YL1/2 Ab (red). Anti-LdCen4 displays the localization of LdCen4 close to the kinetoplast (a region where basal bodies are located [1]). Note LdCen4 in addition to the basal body region also stains lobe(s) like structures close to the basal bodies. DAPI stains nuclei and kinetoplasts. N: nucleus; K: kinetoplast; B: basal body; L: lobe(s). The scale bar is 10 μm in the upper and middle panels and 2 μm in the lower panel.

3.5.2. Confirmation of LmxCen4 knockout by PCR and immunoblotting

PCR amplification of DNA fragment specific for 'Centrin4 knockout' showed amplification in the wild type (Fig. 4B, Lane 14) cell line with specific primers indicated in Fig. 4A & C. However, it was not amplified in the selected LmxCen4 knockout cell line (Fig. 4B, Lane 13). All possible combinations were positive for gene knockout (Fig. 4B rest of lanes). The PCR confirmed the integration of the repair cassettes with neomycin and puromycin drug resistance genes at the right location as per the amplification of the right-sized fragments.

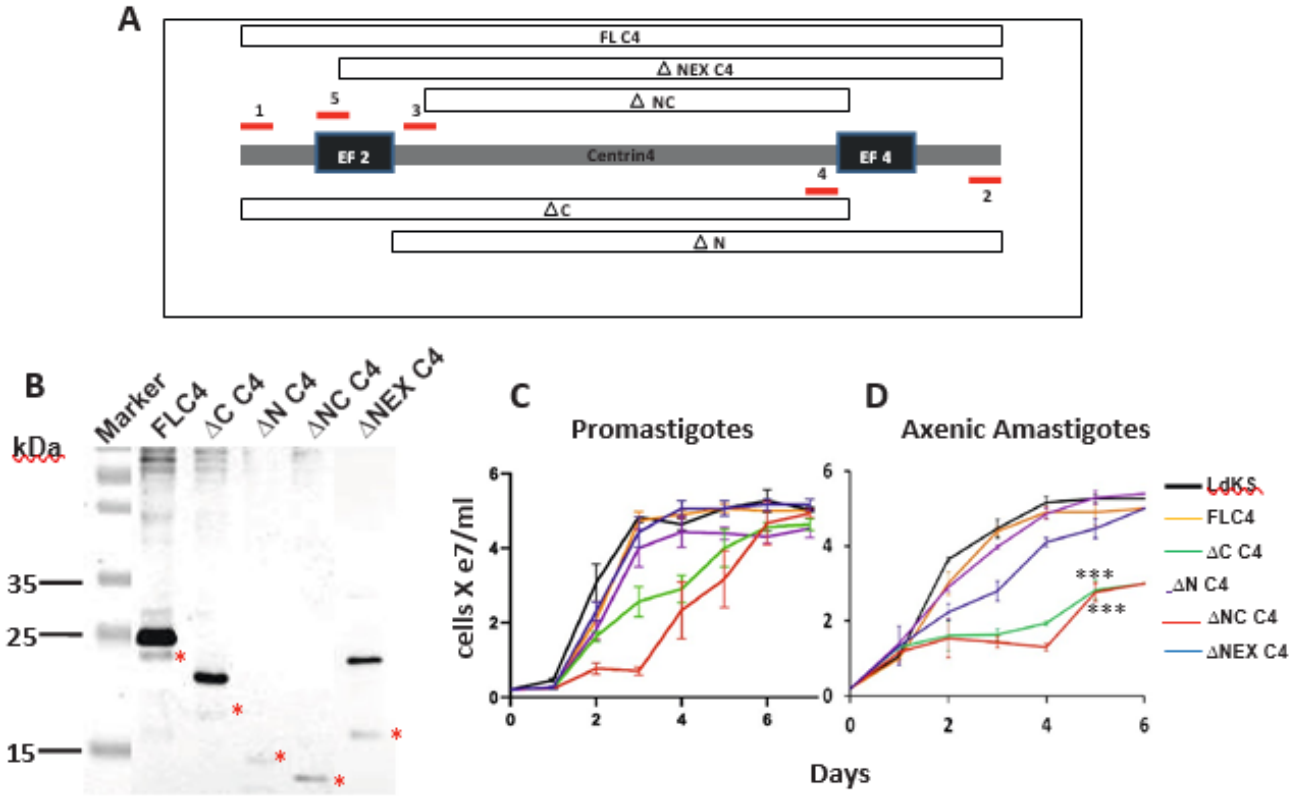

Fig. 3. Growth physiology of episomal expression of mutant centrin proteins in the parasite.

A. Schematic diagram depicting the regions considered for deletion in the LdCen4 during vector construction for episomal expression of truncated proteins in the parasite. B: Western blot analysis using an anti-HA antibody to confirm the overexpressed proteins in the promastigotes after transfection with full- length or mutant constructs of LdCen4 as in 'A' above. The red star indicates the recombinant episomally expressing the protein in each case. A separate blot was run for ΔNEX and the two blots were stitched together. The molecular weight of red star bands in lanes: FL C4: 23.3 kDa; ΔC C4: 20.4 kDa; ΔN C C4: 15.1 kDa; ΔNC C4: 12.2 kDa; ΔNEX C4: 16.5 kDa. C: Growth of Promastigotes episomally expressing the mutant forms of LdCen4. D. Growth of axenic amastigotes episomally expressing the mutant forms of LdCen4. Whereas, EF1 is EF-hand 1 (calcium-binding region 1); EF4 is EF-hand IV (calcium-binding region 4); FL C4 is Full-length LdCen4 of 630 bp; ΔC C4 is C-terminal deleted LdCen4 of 552 bp, ΔN C4 is N-terminal deleted LdCen4 of 408 bp, ΔNEX C4 is N-terminal extended LdCen4 of 447 bp, ΔNC C4 is N and C-terminal deleted LdCen4 of 330 bp. The data at each point was mean ± SE of three independent values. The stars in 'D' signify that they are statistically significant by 'Two-way ANOVA' analysis with the control.

LmxCen4KO cell line was reconfirmed for gene deletion by observing the absence of protein expression in these cells by immunoblotting anti- LdCen4 antibodies. The expression of LmxCen4 protein was clearly observed in the wild-type strain, which increased with the increasing number of cells used. However, the expression of LmxCen4 was not detected even at the higher number of KO cell lysates (Fig. 4D). Further reaffirmation of the knockout was carried out through a Western blot, observing the absence of LmxCen4 expression in the cytoskeletal frac- tion (basal body) of the cell line (Fig. 4E).

3.5.3. LmxCen4 deleted L. mexicana parasites display growth attenuation only in vitro and not ex vivo.

To extrapolate the function of centrin4 in the null background, the physiology of the LmxCen4 deleted *L. mexicana* parasites was further studied. The growth of the knockout parasite as both promastigotes and axenic amastigotes was monitored in culture. The LmxCen4KO cell line showed significantly reduced growth in both the promastigote and amastigote cultures compared to the wild-type controls (Fig. 5A–B). The in vitro infectivity was evaluated with stationary phase LmxCen4KO and wild-type parasites. We found no statistically significant difference in % macrophage infection between the wild-type cells harboring Cas9 construct and LmxCen4KO at 48 hours and 72 hours post-infection in THP-1 human macrophage cells (Fig. 5C & D). Although our in vitro growth study showed slower growth for the LmxCen4KO cells at the amastigote stage of the parasite, surprisingly, we observed the uniform infectivity of KO and control parasites in the macrophages, signifying differential physiology between its growth in vitro and in vivo.

3.6. POC isoforms of *L. donovani* and *L. mexicana* cluster together

POC isoforms of *L. donovani* and *L. mexicana* cluster

together with 94% identity in the dendrogram, suggesting a common phylogenetic origin and a significant homology in the sequences (Fig. 6 A–B). The human POC (HsPOC) was highly divergent from the other genes, protruding distinctly in the cladogram from *Leishmania* and Trypanosoma sp.

3.7. LdCen4 binds to LdPOC

3.7.1. In silico binding interaction between LdCen4 and LdPOC: Accuracy and reliability of modelled LdPOC protein

We carried out in silico analysis to confirm the interaction between LdCen4 and LdPOC. The rank one template (PDB ID: 4cgk chain A) was selected to model LdPOC protein based on heuristics to maximize con- fidence (97.7 %) and alignment coverage (94 %) (Supplementary Table 5). Another table indicates the PDB ID 4cgk chain A alignment coverage by each template, the prediction confidence, the number of matching aa to that template, and overall

information of the PDB ID 4cgk-A (Supplementary Table 6). Of 339 amino acids, only 16 residues were modelled by ab initio, and 95 % of aa residues were modelled with >90 % confidence. The minimum energy of the developed model was 144.629 Kcal/mol (Supplementary Table 6). After the Superposition of the model of POC protein with template PDB ID 4cgk-A, the RMSD between the target and template protein was found to be incredibly low value (0.000 Å) and TM- score exceptionally high (1.00) (Supplementary Table 7). The superimposition of the target-template protein was performed within a threshold size of 3.5 Å. The sequence alignment of model POC protein of *L. donovani* with the template crystal structure of the essential protein PcsB from Streptococcus pneumonia (PDB ID: 4cgk_A) shows that the LdPOC protein is majorly an alpha-loop-alpha protein having eight alpha secondary structure elements (α1-α8) and seven loops (green) (Fig. 7A).

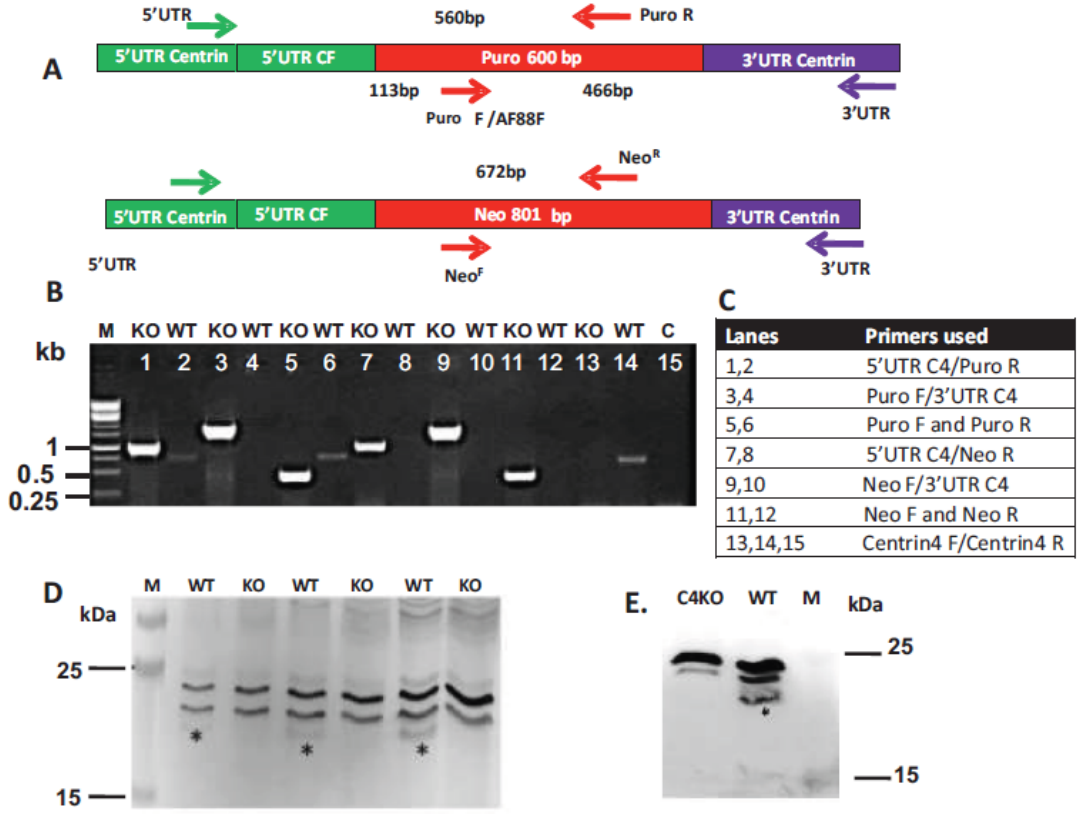

Fig. 4. Confirmation of LmxCen4 knockout cell line:

A. Schematic representation of KO cassette with the information of PCR primers. B. PCR confirmation of LmxCen4KO cell line: Whereas WT: wild type; KO: knockout; C: no template control; C. List of primer combinations used in specific lanes. D: Western blot analysis of LmxCen4 protein in the knockout cell line. The different number of parasite density of wild type and knockout (LmxCen4KO) protein lysate subjected SDS-page WT: wild type, KO: knockout, M: protein marker. E. Western blot of parasite cytoskeletal protein lysate with anti-LdCen4 Ab. In D & E, the black star bands indicate LmxCen4 in the whole-cell lysate of wild type (Wt) *L. mexicana*, which are absent in the knockout cells (LmxCen4KO). In these the other dark bands close to LmxCen4 could be some non-specific binding seen in all, that need to be accessed further.

The eight alpha-helix comprises ~65 % of POC protein, while two beta-sheets and seven loops comprise ~35 % of the modelled POC protein. The amino acid residues from 10 to 200 forming four alpha-helices (α1-α4) is

the core structure, which is modelled in almost the top 20 models of POC protein by Phyre2 tools (Fig. 7A). The Ramachandran plot analysis of energetically most favored regions for amino acid residues of backbone Phi (Φ)/(Psi (Ψ) dihedral angles are observed by three colored contours regions-energetically most favored (dark green), energetically favored (olive green) and additionally allowed region (light grey) (Fig. 7B). The Ramachandran plot of backbone dihedral angles (Φ/Ψ pairs) showed that 90.80 % of amino acids (Supplementary Table 8) come within the first contours line (dark green) of the energetically most favored region (Fig. 7B) of amino acid residues of modelled POC protein. The modelled LdPOC protein was superimposed and compared with the native X-ray crystallographic structure of template essential protein PcsB from Streptococcus pneumoniae (PDB ID: 4cgk_A) in the PyMOL Molecular Graphics System, Version 2.0 (Schrödinger, LLC). The struc- turally validated model of LdPOC protein (magenta) is superimposed with template PDB ID: 4cgk chain A (green) structure for identification of similarities and differences in native X-ray crystallographic and modelled structure of LdPOC protein (Fig. 7C). The ribbon diagrams clearly showed that the four alpha helices (α1-α4) are almost identical in modelled and template protein (Fig. 7C). There is a difference in some alpha helices and the number of loops in modelled and template LdPOC protein, which are shown by red arrows (Fig. 7C). The two 180◦ apart different orientations clearly show the structural differences in modelled (magenta) and template protein (green) (Fig. 7C).

3.7.2. Analysis of a docked complex of modelled LdCen4 and LdPOC proteins

Docking of Centrin4 model.pdb (as a receptor) with POC model.pdb (as a ligand) was performed by ZDOCK version 2.3.2 Fast Fourier Transform-based protein docking

algorithm. The ZDOCK top ten docked complexes of LdCen4 with LdPOC protein were sorted by rank, 3 rota- tional angles and 3 translational parameters, which are enlisted in Supplementary Table 7. Then each pose of the docked complexes was visualized in the PyMOL Molecular Graphics System (Version 2.0 of Schro¨dinger, LLC). The rank first docked pose having three rotational angles, or Euler angles 2, 155, and 18 (in radians) for rotating the ligand and three translational parameters (XYZ grid position) 1.884956, 1.934862 and 1.989776 (in Angstrom) for the ligand concerning its starting point was found best-fitted pose. The PyMOL Molecular Graphics System, confirmed that α1 –α4 alpha-helices of LdPOC protein (red color) interact with α1-α7 helices of Ldcen4 (green) amino acid residues (Fig. 7D). While the closeup view unveils that α1 (GLU15-ARG42), α2 (ALA50-HIS80) and α3 (LEU87-ALA156) helices of LdPOC amino acid residues interacted with α1 (GLU49-PHE62), α2 (PRO71-ALA81) and α3 (SER88-VAL98) helices of LdCen4 amino acid residues. By very close examination of amino acid interaction analysis, it was found that GLU18, ASN28, SER32, ILE35, TYR38, LEU39, ARG42 of α1 helix and LEU135, ALA138, TYR139, TRP142, PHE145 of α3 helix amino acid residues of LdPOC protein (red) is interacting with LYS61, PHE62 of α1 helix, HIS73, VAL76, VAL77, ALA78, TYR80, ALA81 of α2 helix and SER88, ALA89, LEU91, GLN92, GLN93, LEU95, GLN96 of α3 helix amino acid residues of LdCen4 pro- tein (green). Some hydrophobic aa residues of loop regions of LdPOC viz., MET1, GLU7, ASP9, THR43, GLN45, VAL46) and LdCen4 viz., GLU104, GLY175, TYR176, HIS177, ARG205 proteins are also interacting. Meanwhile, these amino acid residues involved in the interaction of LdCen4 with LdPOC proteins were also analyzed using the DIMPLOT module of LigPlot version 1.4.5 [25] and are enlisted in Supplementary Table 8.

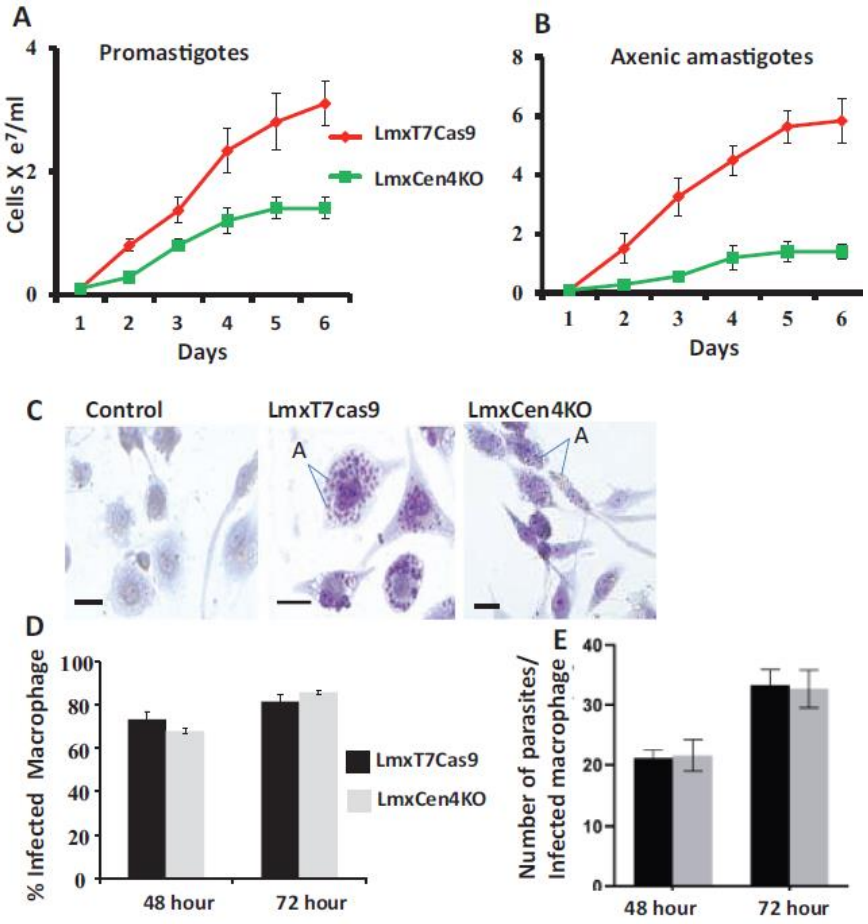

Fig. 5. (A–B): In vitro growth of LmxCen4KO. A. The effect of LmxCen4 disruption in vitro in the growth of promastigotes and axenic amastigotes compared to non-edited parasites (with T7Cas9 construct). The initial cell density taken in the culture was 1x106cells/ml. The data represent the means of SD of three independent experiments. (C–D) Ex vivo infectivity of LmxCen4 null-mutant parasites. THP1 macrophages were infected with either wild-type (with T7Cas9 construct) or LmxCen4 null mutant for 48 and 72 h at a ratio of 10:1 (parasites/macrophage). C. Infected macrophages after 48 h of infection and Giemsa staining. Scale bar: 10 mM. A: axenic amastigotes. D. Bar graph showing the percentage of macrophages infected. Percentages of infected macrophages were determined by counting a minimum of 300 macrophages under a microscope (×100). Values represent mean ± SD from three independent experiments. All data are statistically significant by 'Two way of ANOVA' analysis.

The Surface Cartoon Model of Fig. 7E is also showing amino acids of α1 (GLU15-ARG42) and α3 (LEU87-ALA156) helices of POC protein (red) stringently interacting with amino acid residues of α1 (GLU49- PHE62), α2 (PRO71-ALA81) and α3 (SER88-VAL98) helices of LdCen4 protein (spotted green). The two representations are shown from two different orientations at 180◦ apart (Fig. 7E). There are 22 LdCen4 amino acid residues found interacting with 18 amino acid residues of LdPOC protein. The GLU74 (α1), ARG201 (α7), ARG205 (loop) of LdCen4 protein formed hydrogen and hydrophobic bonds with TYR38 (α1), ARG42 (α1), GLU7 (loop) and ASP9 (loop) of POC protein. The other 19 hydrophobic amino acid residues of LdCen4 protein formed hydrophobic bonds with 15 amino acids of LdPOC proteins (Supple- mentary Fig. 1). The interaction of LdCen4 with LdPOC was also confirmed using structural determination by AlfphaFold program as described separately in the 'supplemental section' (Supplementary Figs. 3–6 and Supplementary Tables 9 and 10).

3.7.3. Confirmation of binding of LdCen4 with LdPOC by protein-pulldown assay

GST fused recombinant LdPOC protein expression was confirmed by Western blotting using an Anti-GST antibody (Sigma) (Fig. 8A). Further association of LdPOC with LdCen4 was shown by a pull-down assay. The bead LdPOC-GST associated proteins complex was subjected to SDS- PAGE and Western blotting using either anti-LdCen4 or anti-GST anti-bodies. LdCen4 protein band was observed at 25 kDa (panel 2), sug- gesting the LdCen4 association with LdPOC protein in the parasite (Fig. 8B).

3.7.4. Centrin 4 binding to LdPOC is calcium sensitive

The interaction between centrin4 and its binding part-

ner LdPOC was calcium sensitive, as observed by a thick band in the presence of calcium, using anti-LdCen4 antibodies (Fig. 8C). However, the interaction intensity was almost doubled upon the addition of calcium (Fig. 8D).

3.8. Episomal expression of LdPOC in *L. donovani* did not affect parasite growth in vitro

To see the effect of overexpression of LdPOC in the physiology of *L. donovani* parasites and look for any dominant-negative effect in growth, LdPOC was episomally expressed in the parasite through pKSNeo plasmid [1] (Fig.9A). The neomycin-resistant clonal cell line (LdPOC--OE) was monitored for its growth in vitro. The growth of the promastigotes in vitro displayed slightly enhanced growth compared to empty vector-transfected control parasites (Fig. 9B). Consequently, to see its effect on LdPOC-OE cells in the macrophage cell line J774, the parasites were infected ex-vivo in the macrophages and monitored the parasite number after 48 h time point. The host cells infected with LdPOC overexpressor or control parasite in 1:10 ratio showed a marginal increase in the number of LdPOC overexpressing parasites/macrophages compared to control (Fig. Supplementary Fig. 2).

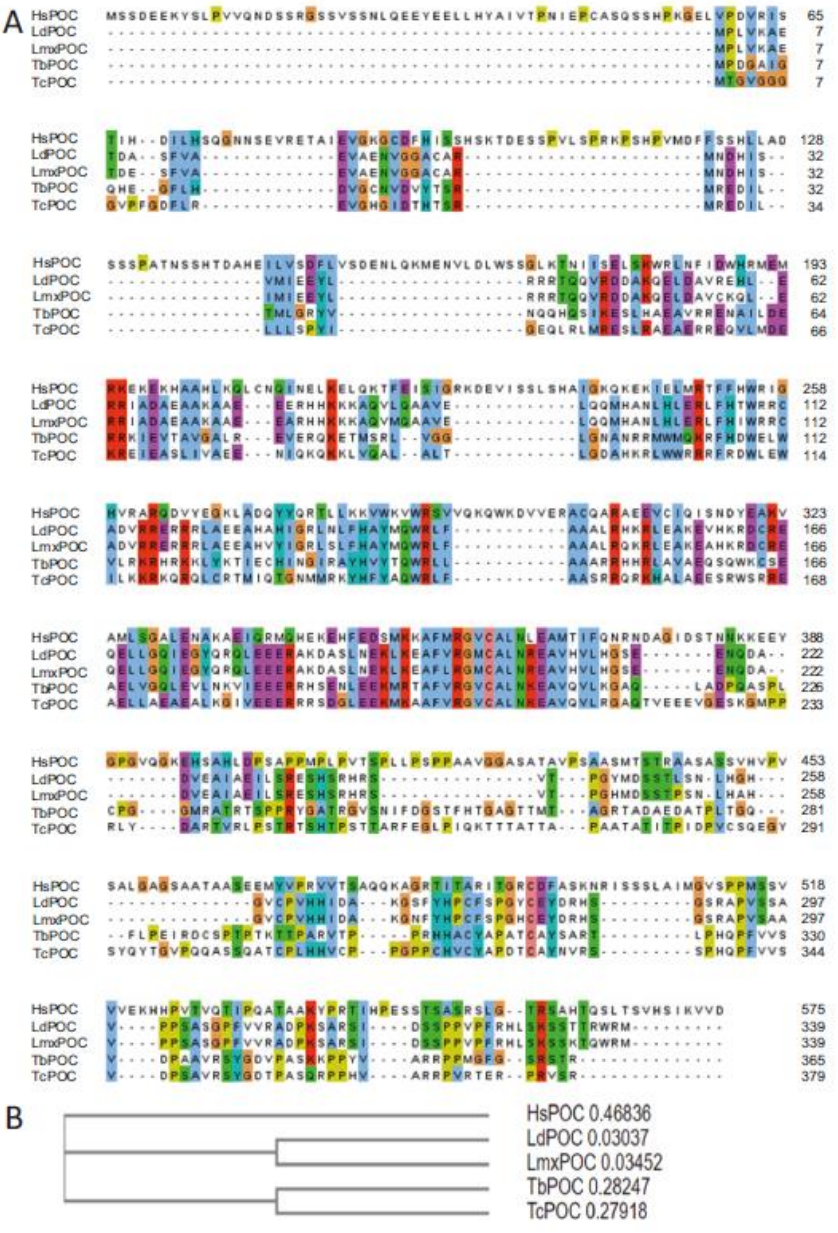

Fig. 6. LdPOC sequence analysis.

A. Multiple alignment of POC protein sequences of HsPOC (NP_001092741.1), LdPOC (XP_003865398.1), LmxPOC (XP_003874621.1), TbPOC (Tb927. 10.7600), TcPOC (TcCLB.510105.190). The alignment was generated utilizing Jalview program version 2.11.2.4. The standard one-letter code is used to define amino acids. The colored patches indicate the respective stretch of amino acids' similarities among the se- quences. B. Phylogenetic analysis of POC ho- mologs. The phylogenetic tree was generated from (nearly conserved) the protein sequences of closely related organisms and species by Neighbor-Joining distance analysis [32].

3.9. LdCen4 and LdPOC are co-localized at the basal body of *L. donovani*

After observing the LdCen4 protein found in the basal body region of *Leishmania* parasites, we aimed to see

the localization of LdPOC. LdPOC was found to be localized at the basal body region as per the co-IFA using anti-LdCen1 Ab (known to localize at the basal body region; [1]) and anti-HA Ab (to localize LdPOC-HA) in the LdPOC-OE cells (Fig. 9D) with a separate control set having only the secondary antibodies (Fig. 9C). In addition to the basal body region, we have also observed that the anti- HA Ab is also stained at the cytosol region (Fig. 9D). Co-localization studies of LdPOC-HA with LdCen4 in LdPOC-OE *Leishmania* parasite revealed that LdPOC localized at the same region, where Centrin 4 localized at the basal body region (Fig. 9E). But LdPOC was not observed at the lobe structure, where LdCen4 also observed.

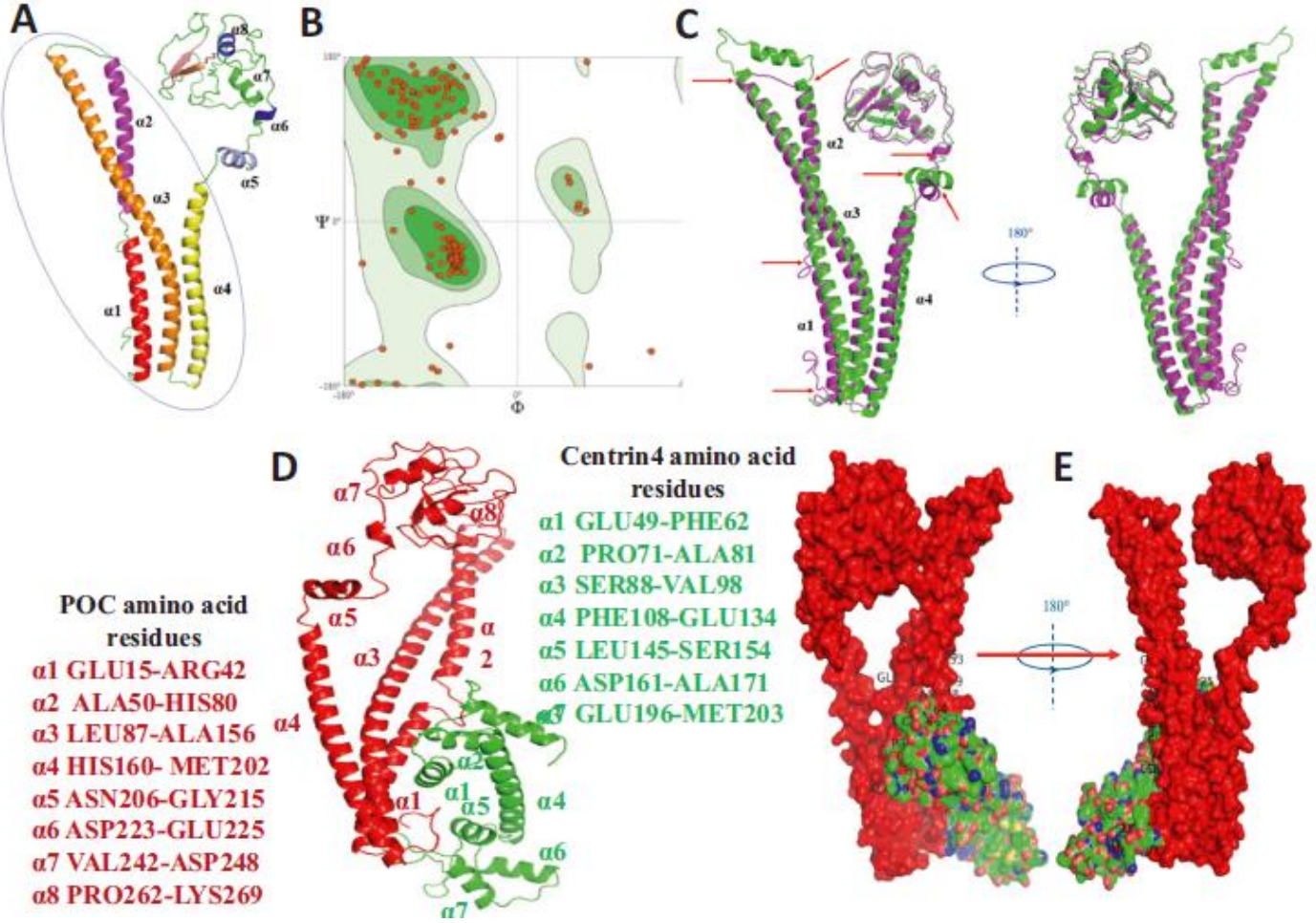

Fig. 7. The modelled LdPOC and the docking study showing its interaction with LdCen4. A. Modelled LdPOC protein of *L. donovani* (spectrum colors) shows the eight alpha helices (α1-α8) and seven loops (green color). The encircled region (blue line) from amino acid 10 to 200 showing four alpha-helices forms the core structure, which is modelled by Phyre2 tools in almost the top 20 models of LdPOC protein. B. Ramachandran plot showing observed backbone dihedral angles (Φ/Ψ pairs) of three colored contours lines of energetically most favored (dark green), favored (olive green) and additionally allowed (light grey) regions of amino acid residues of modelled LdPOC protein. C. Superimposition of LdPOC protein model (magenta) with template PDB ID: 4cgk_A (green) structure showing the similarities and differences in X-ray crystallographic and modelled alpha-loop-alpha secondary structures of LdPOC protein. The four alpha-helices (α1-α4) are almost identical in modelled and template protein, while red arrows show the other structural differences. The two representations are shown from two different orientations at 180◦ apart. D. The docking images showing the interaction between LdCen4 and LdPOC. The docked complex shows alpha-loop-alpha structures of LdCen4 (green) and LdPOC proteins (red) E. The closeup view of α1 (GLU15-ARG42), α2 (ALA50-HIS80) and α3 (LEU87-ALA156) helices of LdPOC amino acid residues interacting with α1 (GLU49-PHE62), α2 (PRO71-ALA81) and α3 (SER88-VAL98) helices of LdCen4 amino acid residues.

4. Discussion

The characterization of cell division proteins in *Leishmania* holds great significance in understanding their cell biology and identifying potential targets for therapeutic intervention and vaccine development, in addition to the regulation of centrin by its binding partners. LdCen4 clusters together with LmCen4, probably in the likelihood of possessing unique EF-hand III together with EF hand-

I. Unlike other centrins of genus Trypanosomes and *Leishmania* (centrin 1–3), which have two calcium-binding EF domains (EF I and IV), centrin4 purportedly lacks this efficient calcium-binding EF-hand IV [8]. The presence of negatively charged amino acids: aspartic acid or glutamic acid in the EF-hand I and III consensus region only, provides two oxygens to coordinate Ca2+ binding further corroborates our supposition of these two as the Ca2+ binding domains in centrin4 [33,34]. There was a report showing >9 fold centrin4 mRNA abundance in the axenic amastigotes compared to promastigotes measured by microarray reported in www.tritrypdb.org for L. infantum (VL causing parasite and genetically a close ally of *L. donovani*) (accession number LINF_320011900) [35]. However, we observed that the LdCen4 protein was found to express equally at both promastigote and axenic amastigote stages (with our laboratory- established culture procedures known to express 'A1' amastigote stage-specific gene/proteins [4,19,36,37]) suggesting its equal importance to these stages of the parasite. This is similar to the expression of LdCen1 protein equally in both the stages in this parasite, despite its promastigote stage-specific mRNA expression [1]. These studies clearly confirm the discrepancy between expression levels of mRNA and the proteins in the parasite suggesting the involvement of the post- transcriptional regulatory mechanism observed in *Leishmania* para- sites, which has also been described by others [38]. Centrins have earlier been reported to be localized in the basal-body region of Chlamydomonas [39], *Leishmania* [1], Paramecium [40] and *T. brucei* [8,41]. LdCen4, like LdCen1 of *L. donovani* and TbCen2 of *T. brucei*, was confirmed to be localized in the basal body of the parasite by immunofluorescence analysis [1,41]. We also found that LdCen4 in addition to the basal body also is observed at the lobe-like structures near the basal body resem- bling *T. brucei* Cen2's dual localization in the basal body and at the bilobed structure [41]. This signifies a potential additional role for LdCen4 in the parasite. It is also noted that the bilobed structure in TbCen2 is close to the golgi apparatus and the deletion of TbCen2 by RNAi also affected the biogenesis of golgi in addition to the basal bodies in *T. brucei* [41]. This was in contrast with the report for the LdCen4 homolog in *T. brucei*, where it is localized throughout the cytosol, nu- cleus and enriched in the flagellum [42], indicating the possible centrin's organism specific roles. Although Centrin2 and 3 were not studied in *L. donovani*, we studied their homologs in *T. brucei* and found that they were involved in organelle segregation without studying at their cellular localization [8,9].

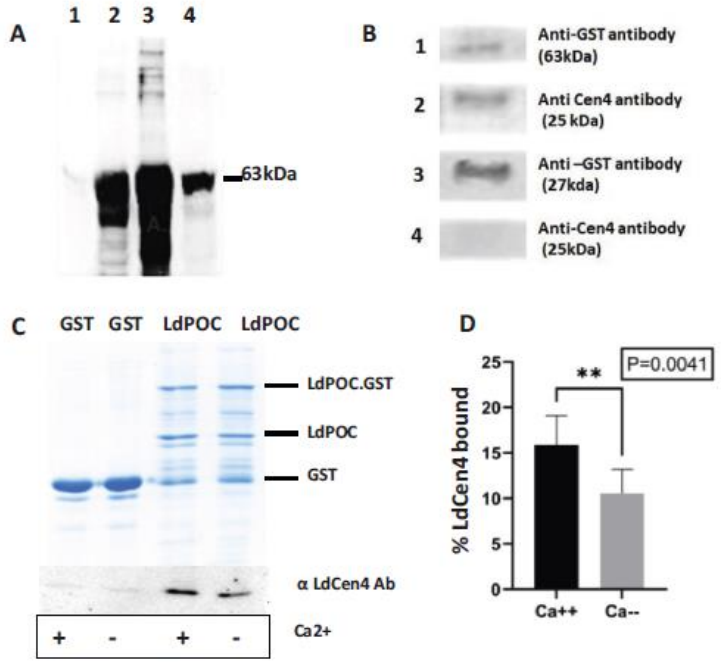

Fig. 8. Confirmation of purified rLdPOC-GST protein in E. coli Rosetta cells by Western blotting using an anti-GST antibody.

A. Lane 1: Uninduced cell lysate; Lane 2: Induced cell lysate; Lane 3: Insoluble proteins of cells overexpressing LdPOC-GST protein; Lane 4: Soluble proteins of cells overexpressing LdPOC-GST protein. B. Confirmation of LdPOC protein by pull- down assay. Panels 1 & 2 represent the LdPOC-GST protein after incubation with *L. donovani* lysate in the pull-down assay went through SDS-PAGE and Western blot. Whereas panels 3 & 4 were similarly processed as in panels 1 & 2 but with only GST protein as the assay control. Western blot with anti-LdCen4 Ab only shows up pulled down of LdCen4 in the process in panel 2 and not in panel 4, explaining the re- action of LdPOC with LdCen4. Western blot with anti- GST Ab displays positivity in panels 1 and 3. C. Cal- cium requirement in the interaction between LdCen4 and LdPOC. GST-pull-down assays were performed with the indicated LdPOC- GST-fusion proteins or with GST alone. The proteins bound to the Glutathione beads were incubated with rLdCen4 in the presence or absence of Ca2+ ions. After washing, the bound pro- teins were separated by SDS–PAGE and stained with Coomassie blue (Upper panel). Another gel with the same loading pattern was used for Western blotting with anti-LdCen4 antibodies to detect the retained LdCen4 protein (lower panel). D. The calcium-dependent binding efficiency of LdCen4 with LdPOC is shown. The data were mean ± SE of three independent experiments. The data is statistically significant with ** p value = 0.0041.

The episomal overexpression of full-length or mutant forms of LdCen4 protein exhibited no significant effect on the parasite's growth pattern. In contrast, a reduced growth rate compared to vector- transfected controls in the parasite was observed with the expression of C-terminus truncated proteins, suggesting a dominant negative effect of the truncated proteins, implying a potential role of the C-terminal domain in parasite pathogenesis. Previously, the N-terminal of LdCen1 was essential for the growth of *L. donovani* in vitro [1]. The discrepancy in the functional location in the proteins between LdCen1 and LdCen4 needs to be investigated in the *Leishmania* parasite. Conversely, a significant retarded growth of *L. mexicana* was observed in centrin4 null mutants, generated by the CRISPR Cas9 approach, with about 2 fold decrease in the growth of promastigotes and about 5 fold decrease in amastigotes in vitro, implying its role in cell growth. Reduced growth in vitro was also observed with the TbCen1 and 2 knock-down *T. brucei* via RNAi approach [41]. Our developed *L. donovani* deleted for LdCen1 interestingly displayed attenuated growth in vitro, ex vivo and in vivo in the animals only in the amastigote stage of the parasite, suggesting the relevance LdCen1 protein in the axenic and intracellular amastigote stage of the parasite and protected the animals immunized with LdCenKO cells from virulent challenge [4,11,12]. However, surprisingly, no change in infectivity was observed in the replication of LmxCen4KO ex vivo in the host cells implying differential observation of replication of the parasite's growth in vitro and ex vivo. Hence such parasite's survival was not studied in the animals. Further, LdPOC, a homolog of hPOC in *L. donovani*, has been shown to co-localize with LdCen4 in the basal body of the parasite in addition in the cytosol. For the LdPOC localization, we relied on the localization of the overexpressing LdPOC-HA using anti-HA Ab. In our future studies anti-POC antibodies (under development) may be used to stain the endogenous LdPOC protein to know its

actual placement in the cell. The role of LdPOC in the assembly of complete centrioles and cell prolifer- ation, like hPOC5, can be ascertained by increased cellular proliferation and increased virulence patterns in overexpressing parasites [25]. The presence of a tandem repeat of centrin-binding sequences and the short coiled-coil regions in LdPOC, like its homologs (hPOC), helps in binding with centrin. This is similar to the already reported interaction between hPOC5 and hCen2 and hCen3 [25]. This is the first report of a *Leishmania* centrin binding partner. The Molecular docking approach by ZDOCK further ascertained this binding pattern using the LdPOC model generated ab initio. The PyMOL Molecular Graphics System confirmed that α1–α4 alpha-helices of LdPOC protein interact with α1-α7 helices of LdCen4 amino acid resi- dues. Stringent interaction between the residues of α1 to 3 of LdCen4 with that of α1 and 3 residues of LdPOC was observed. Also, GLU74 (α1), ARG201 (α7) and ARG205 (loop) of LdCen4 protein formed hydrogen and hydrophobic bonds with TYR38 (α1), ARG42 (α1), GLU7 (loop) and ASP9 (loop) of LdPOC protein, confirming helix and loop interaction between them. In total, about 22 LdCen4 amino acid residues were found to be interacting with 18 amino acid residues of POC protein. Thus, another new calcium-binding protein, centrin4, has been characterized in *Leishmania* sp. describing its property and basal body localization, similar to its earlier reported counterpart centrin1. This report also brings to light the predicted structural details of LdCen4's novel calcium dependent interacting partner LdPOC, which also co- localises with LdCen4, although only at the basal body region and not at the lobe-like structure(s). The putative amino acids of both the pro- teins that are involved in the interaction have been predicted. This report could help open new avenues in research, exploring the role on the interaction between these macromolecules, potentially towards novel therapeutics against the tropical diseases due to protozoan parasites.

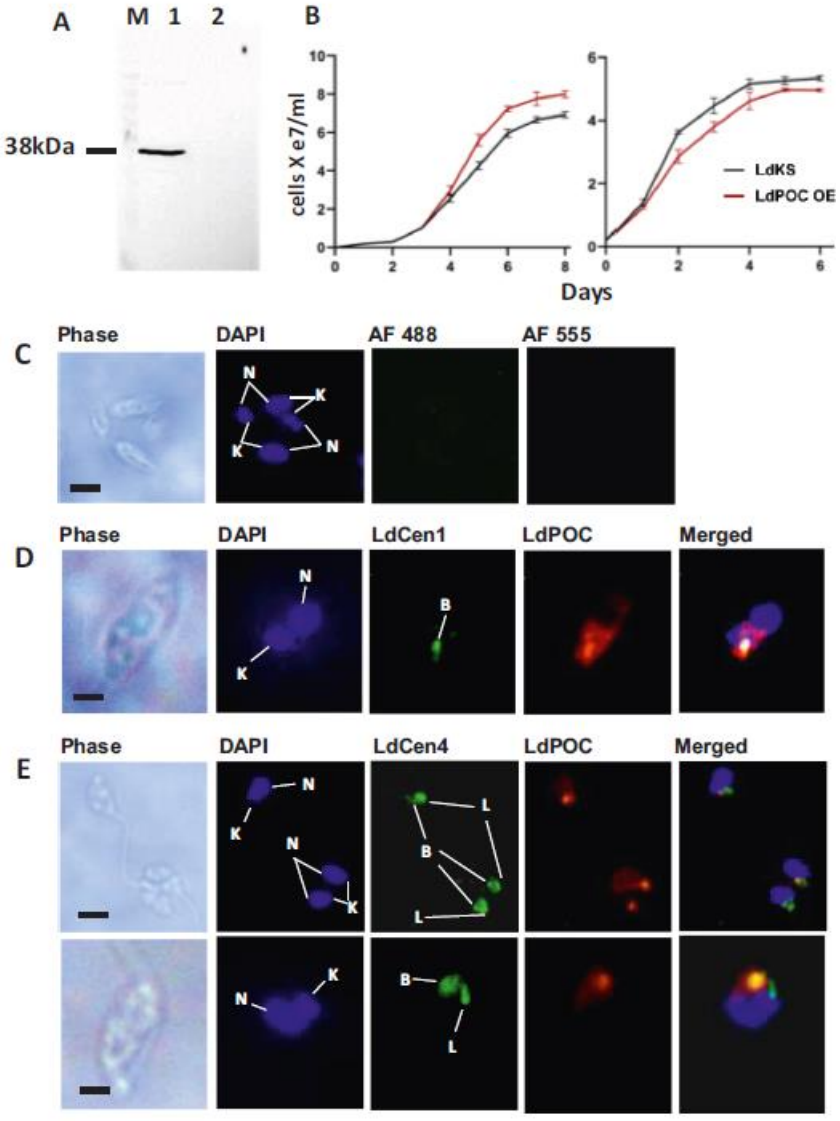

Fig. 9. Growth physiology of episomal LdPOC expression in *L. donovani* (A & B). A. Confirmation of expression of LdPOC-HA by Western blotting. Lane M: Protein ladder, Lane 1: whole cell lysate protein of *L. donovani* overexpressing LdPOC-HA; Lane 2: whole cell lysate of *L. donovani* with pKSNeo as transfected control. B. Growth curve analysis of LdPOC overexpression versus pKSNeo control *L. donovani* parasites. No significant growth difference was observed between LdKS and LdPOC-HA overexpressing parasites, both in the promastigote and amastigote stages. Colocalization of LdPOC with LdCen4 in *L. donovani* parasites (C–F) C. Control immunofluorescence without immune sera and with only the secondary antibodies. D. Localization of LdPOC-HA in the LdPOC overexpressing promastigotes using anti-HA antibodies and the known basal body associated anti-Centrin1 antibodies [1]. E. Colocalization LdCen4 (green) with anti-LdCen4 antibodies and LdPOC-HA (red) with anti-HA antibodies and the merged (blue, green and red) image in the promastigote (upper panel with 3 cells and lower panel with a different single enlarged cell). Yellow dots indicate that LdCen4 (Green) and LdPOC (Red) co-localize within the parasite at the basal body region. The other lobe region stained by anti-LdCen4 antibodies that is not localized by LdPOC-HA is also observed. N is the nucleus; K is the kinetoplast; B is the basal body; L is the lobe (s). The scale bar is 5 μm in panels C and E upper panel and 2 μm in panels D and E lower panel.

Credit authorship contribution statement

KV, RT and THW: Investigation. KV, RT and MSB: Writing original draft. MAB, R, RMC, AKY: Methodology. MSB: Computer simulation, AK and NP: Study support and manuscript editing. AC, PS, YS and AS: Study support and supervision.

Declaration of competing interest

The authors have no conflicts of interest to declare.

Data availability

All the data are already mentioned in the manuscript.

Acknowledgement

AS and NP were funded by Indian Council of Medical Research, India (GIA/2/VBD/2021/ECD-II) and Science and Engineering Research Board, Department of Science and Technology, India (EMR/2015/ 000874), Government of India. AY and RMC were funded by the French LabEx ParaFrap (ANR-11-LABX-0024). KV was supported by DST- INSPIRE (IF140108) Government of India and EMBO Short term fellowship (STF-7207). RT was supported by DST-SERB (PDF/2015/ 000768), Government of India.

Appendix A. Supplementary data

Supplementary data to this article can be found online at https://doi. org/10.1016/j.bbamcr.2022.119416.

References

[1] A. Selvapandiyan, R. Duncan, A. Debrabant, S. Bertholet, G. Sreenivas, N.S. Negi, P. Salotra, H.L. Nakhasi, Expression of a mutant form of leishmania donovani centrin reduces the growth of the parasite, J. Biol. Chem. 276 (2001) 43253–43261.

[2] S. Veeraraghavan, P.A. Fagan, H. Hu, V. Lee, J.F. Harper, B. Huang, W.J. Chazin, Structural independence of the two EF-hand domains of caltractin, J. Biol. Chem. 277 (2002) 28564–28571.

[3] J.L. Salisbury, K.M. Suino, R. Busby, M. Springett, Centrin-2 is required for centriole duplication in mammalian cells, Curr. Biol. 12 (2002) 1287–1292.

[4] A. Selvapandiyan, A. Debrabant, R. Duncan, J. Muller, P. Salotra, G. Sreenivas, J. L. Salisbury, H.L. Nakhasi, Centrin gene disruption impairs stage-specific basal body duplication and cell cycle progression in leishmania, J. Biol. Chem. 279 (2004) 25703–25710.

[5] P. Trojan, N. Krauss, H.W. Choe, A. Giessl, A. Pulvermuller, U. Wolfrum, Centrins in retinal photoreceptor cells: regulators in the connecting cilium, Prog. Retin. Eye Res. 27 (2008) 237–259.

[6] O. Gavet, C. Alvarez, P. Gaspar, M. Bornens, Centrin4p, a novel mammalian centrin specifically expressed in ciliated cells, Mol. Biol. Cell 14 (2003) 1818–1834.

[7] B. Mahajan, A. Selvapandiyan, N.J. Gerald, V. Majam, H. Zheng, T. Wickramarachchi, J. Tiwari, H. Fujioka, J.K. Moch, N. Kumar, L. Aravind, H. L. Nakhasi, S. Kumar, Centrins, cell cycle regulation proteins in human malaria parasite plasmodium falciparum, J. Biol. Chem. 283 (2008) 31871–31883.

[8] A. Selvapandiyan, P. Kumar, J.C. Morris, J.L. Salisbury, C.C. Wang, H.L. Nakhasi, Centrin1 is required for organelle segregation and cytokinesis in *Trypanosoma brucei*, Mol. Biol. Cell 18 (2007) 3290–3301.

[9] A. Selvapandiyan, P. Kumar, J.L. Salisbury, C.C. Wang, H.L. Nakhasi, Role of centrins 2 and 3 in organelle segregation and cytokinesis in trypanosoma brucei, PLoS One 7 (2012), e45288.

[10] A. Selvapandiyan, R. Dey, S. Gannavaram, S. Solanki, P. Salotra, H.L. Nakhasi, Generation of growth arrested leishmania amastigotes: a tool to develop live attenuated vaccine candidates against visceral leishmaniasis, Vaccine 32 (2014) 3895–3901.

[11] A. Selvapandiyan, R. Dey, S. Nylen, R. Duncan, D. Sacks, H.L. Nakhasi, Intracellular replication-deficient leishmania donovani induces long lasting protective immunity against visceral leishmaniasis, J. Immunol. 183 (2009) 1813–1820.

[12] J.A. Fiuza, S. Gannavaram, C. Santiago Hda, A. Selvapandiyan, D.M. Souza, L. S. Passos, L.Z. de Mendonca, S. Lemos-Giunchetti Dda, N.D. Ricci, D. C. Bartholomeu, R.C. Giunchetti, L.L. Bueno, R. Correa-Oliveira, H.L. Nakhasi, R. T. Fujiwara, Vaccination using live attenuated leishmania donovani centrin deleted parasites induces protection in dogs against leishmania infantum, Vaccine 33 (2015) 280–288.

[13] P. Bhattacharya, R. Dey, P.K. Dagur, A.B. Joshi, N. Ismail, S. Gannavaram, A. Debrabant, A.D. Akue, M.A. KuKuruga, A. Selvapandiyan, J.P. McCoy Jr., H. L. Nakhasi, Live attenuated leishmania donovani centrin Knock out parasites generate non-inferior protective immune response in aged mice against visceral leishmaniasis, PLoS Negl. Trop. Dis. 10 (2016), e0004963.

[14] G. Volpedo, P. Bhattacharya, S. Gannavaram, T. Pacheco-Fernandez, T. Oljuskin, R. Dey, A.R. Satoskar, H.L. Nakhasi, The history of live attenuated centrin gene- deleted leishmania vaccine candidates, Pathogens 11 (2022).

[15] J.V. Kilmartin, Sfi1p has conserved centrin-binding sites and an essential function in budding yeast spindle pole body duplication, J. Cell Biol. 162 (2003) 1211–1221.

[16] R. Nishi, Y. Okuda, E. Watanabe, T. Mori, S. Iwai, C. Masutani, K. Sugasawa, F. Hanaoka, Centrin 2 stimulates nucleotide excision repair by interacting with xeroderma pigmentosum group C protein, Mol. Cell. Biol. 25 (2005) 5664–5674.

[17] T.J. Dantas, O.M. Daly, P.C. Conroy, M. Tomas, Y. Wang, P. Lalor, P. Dockery, E. Ferrando-May, C.G. Morrison, Calcium-binding capacity of centrin2 is required for linear POC5 assembly but not for nucleotide excision repair, PLoS One 8 (2013), e68487.

[18] T. Beneke, R. Madden, L. Makin, J. Valli, J. Sunter, E. Gluenz, A CRISPR Cas9 high- throughput genome editing toolkit for kinetoplastids, R. Soc. Open Sci. 4 (2017), 170095.

[19] K. Ahuja, M.A. Beg, R. Sharma, A. Saxena, N. Naqvi, N. Puri, P.K. Rai, A. Chaudhury, R. Duncan, P. Salotra, H. Nakhasi, A. Selvapandiyan, A novel signal sequence negative multimeric glycosomal protein required for cell cycle progression of *Leishmania donovani* parasites, Biochim. Biophys. Acta, Mol. Cell Res. 1865 (2018) 1148–1159.

[20] K. Ahuja, G. Arora, P. Khare, A. Selvapandiyan, Selective elimination of leptomonas from the in vitro co-culture with leishmania, Parasitol. Int. 64 (2015) 1–5.

[21] W.W. Zhang, H. Charest, E. Ghedin, G. Matlashewski, Identification and overexpression of the A2 amastigote-specific protein in leishmania donovani, Mol. Biochem. Parasitol. 78 (1996) 79–90.

[22] K.A. Robinson, S.M. Beverley, Improvements in transfection efficiency and tests of RNA interference (RNAi) approaches in the protozoan parasite leishmania, Mol. Biochem. Parasitol. 128 (2003) 217–228.

[23] R.M. Corrales, S. Vaselek, R. Neish, L. Berry, C.D. Brunet, L. Crobu, N. Kuk, J. Mateos-Langerak, D.R. Robinson, P. Volf, J.C. Mottram, Y. Sterkers, P. Bastien, The kinesin of the flagellum attachment zone in leishmania is required for cell morphogenesis, cell division and virulence in the mammalian host, PLoS Pathog. 17 (2021), e1009666.

[24] G. Schumann Burkard, P. Jutzi, I. Roditi, Genome-wide RNAi screens in bloodstream form trypanosomes identify drug transporters, Mol. Biochem. Parasitol. 175 (2011) 91–94.

[25] J. Azimzadeh, P. Hergert, A. Delouvee, U. Euteneuer, E. Formstecher, A. Khodjakov, M. Bornens, hPOC5 is a centrin-binding protein required for assembly of full-length centrioles, J. Cell Biol. 185 (2009) 101–114.

[26] N. Sahoo, J. Troger, S.H. Heinemann, R. Schonherr, Current inhibition of human EAG1 potassium channels by the Ca2 binding protein S100B, FEBS Lett. 584 (2010) 3896–3900.

[27] M.S. Baig, E. Reyaz, A. Selvapandiyan, A. Krishnan, Differential binding of SARS- CoV-2 spike protein variants to its cognate receptor hACE2 using molecular modeling based binding analysis, Bioinformation 17 (2021) 337–347.

[28] V. Sharma, P. Sharma, A. Selvapandiyan, P. Salotra, *Leishmania donovani*-specific Ub-related modifier-1: an early endosome-associated ubiquitin-like conjugation in *Leishmania donovani*, Mol. Microbiol. 99 (2016) 597–610.

[29] R.A. Laskowski, M.B. Swindells, LigPlot : multiple ligand-protein interaction diagrams for drug discovery, J. Chem. Inf. Model. 51 (2011) 2778–2786.

[30] C.J. Sigrist, L. Cerutti, E. de Castro, P.S. Langendijk-Genevaux, V. Bulliard, A. Bairoch, N. Hulo, PROSITE, a protein domain database for functional characterization and annotation, Nucleic Acids Res. 38 (2010) D161–D166.

[31] N.S. Kron, In search of the aplysia immunome: an in silico study, BMC Genomics 23 (2022) 543.

[32] S. Ahmad, A. Selvapandiyan, R.K. Bhatnagar, Phylogenetic analysis of gram-positive bacteria based on grpE, encoded by the dnaK operon, Int. J. Syst. Evol. Microbiol. 50 (Pt 5) (2000) 1761–1766.

[33] I. Durussel, Y. Blouquit, S. Middendorp, C.T. Craescu, J.A. Cox, Cation- and peptide-binding properties of human centrin 2, FEBS Lett. 472 (2000) 208–212.

[34] L. Bombardi, M. Pedretti, C. Conter, P. Dominici, A. Astegno, Distinct calcium binding and structural properties of two centrin isoforms from toxoplasma gondii, Biomolecules 10 (2020).

[35] T. Lahav, D. Sivam, H. Volpin, M. Ronen, P. Tsigankov, A. Green, N. Holland, M. Kuzyk, C. Borchers, D. Zilberstein, P.J. Myler, Multiple levels of gene regulation mediate differentiation of the intracellular pathogen *Leishmania*, FASEB J. 25 (2011) 515–525.

[36] K. Avishek, K. Ahuja, D. Pradhan, S. Gannavaram, A. Selvapandiyan, H.L. Nakhasi, P. Salotra, A leishmania-specific gene upregulated at the amastigote stage is crucial for parasite survival, Parasitol. Res. 117 (2018) 3215–3228.

[37] G. Sreenivas, R. Singh, A. Selvapandiyan, N.S. Negi, H.L. Nakhasi, P. Salotra, Arbitrary-primed PCR for genomic fingerprinting and identification of differentially regulated genes in indian isolates of leishmania donovani, Exp. Parasitol. 106 (2004) 110–118.

[38] S. Haile, B. Papadopoulou, Developmental regulation of gene expression in trypanosomatid parasitic protozoa, Curr. Opin. Microbiol. 10 (2007) 569–577.

[39] J.L. Salisbury, Centrin, centrosomes, and mitotic spindle poles, Curr. Opin. Cell Biol. 7 (1995) 39–45.

[40] F. Ruiz, N. Garreau de Loubresse, C. Klotz, J. Beisson, F. Koll, Centrin deficiency in paramecium affects the geometry of basal-body duplication, Curr. Biol. 15 (2005) 2097–2106.

[41] C.Y. He, M. Pypaert, G. Warren, Golgi duplication in *Trypanosoma brucei* requires Centrin2, Science 310 (2005) 1196–1198.

[42] F. Shan, X. Yang, Y. Diwu, H. Ma, X. Tu, *Trypanosoma brucei* centrin5 is enriched in the flagellum and interacts with other centrins in a calcium-dependent manner, FEBS Open Bio 9 (2019) 1421–1431.